NANO LETTERS

2008
Vol. 8, No. 7
1858-1865

Cellular Trafficking of Quantum Dot-Ligand Bioconjugates and Their Induction of Changes in Normal Routing of Unconjugated Ligands

Christina Tekle,[†,‡] Bo van Deurs,[§] Kirsten Sandvig,[†,‡] and Tore-Geir Iversen*[,†,‡]

Centre for Cancer Biomedicine, Faculty Division, Norwegian Radium Hospital, University of Oslo, 0316 Oslo, Norway, Institute for Cancer Research, Department of Biochemistry, Norwegian Radium Hospital, Rikshospitalet University Hospital Montebello, 0310 Oslo, Norway, and Department of Cellular and Molecular Medicine, University of Copenhagen, The Panum Institute, 2200 Copenhagen N, Denmark

ABSTRACT

Can quantum dots (Qdots) act as relevant intracellular probes to investigate routing of ligands in live cells? The intracellular trafficking of Qdots that were coupled to the plant toxin ricin, Shiga toxin, or the ligand transferrin (Tf) was studied by confocal fluorescence microscopy. The Tf:Qdots were internalized by clathrin-dependent endocytosis as fast as Tf, but their recycling was blocked. Unlike Shiga toxin, the Shiga:Qdot bioconjugate was not routed to the Golgi apparatus. The internalized ricin:Qdot bioconjugates localized to the same endosomes as ricin itself but could not be visualized in the Golgi apparatus. Importantly, we find that the endosomal accumulation of ricin:Qdots affects endosome-to-Golgi transport of both ricin and Shiga toxin: Transport of ricin was reduced whereas transport of Shiga toxin was increased. In conclusion, the data reveal that, although coupling of Qdots to a ligand does not necessarily change the endocytic pathway normally used by the ligands studied, it appears that the ligand-coupled Qdot nanoparticles can be arrested within endosomes and somehow perturb the normal endosomal sorting in cells. Thus, the results demonstrate that Qdots may have severe consequences on cell physiology.

Nanoparticles hold a great potential for targeted delivery of small molecules, peptides, and nucleic acids to specific organelles at the cellular level, and as probes in cellular imaging techniques. Quantum dots (Qdots, QDs) are fluorescent semiconductor nanocrystals characterized by their uniform size, size-dependent narrow emission bands, extreme brightness and extended photostability.[1] Research on Quantum dots have evolved into biological applications with potentials for the study of intracellular processes at the single-molecule level, high-resolution live cell imaging, long-term in vivo observation of cell trafficking, and tumor targeting and diagnostics.[2,3] Cytotoxicity of Qdots has been studied, focusing on the effects of leaching of harmful metals from their nanocrystal core, the effects of different surface coatings on cell viability, and on their ability to induce generation of reactive oxygen species (ROS).[4,5] Qdots bound to receptors such as glycine and epidermal growth factor (EGF) receptors have been used to measure and resolve the dynamics of single receptors at the cell surface.[6,7] Except for a few recent studies, little information has been published about the mechanisms of intracellular trafficking of different Qdot-bound ligands.[8–10]

There are still a number of questions about the fate of these particles after they are bound to cells that have to be answered in connection with their use in cell biological studies and certainly before applying them in humans. For instance, if they become associated with cells: To what extent are they internalized? Can they be recycled (sent out of the cell again), or do they become degraded by the cell? If they accumulate, to what extent do they disturb trafficking of natural ligands, and do they have a toxic effect on cells? "Endocytosis" encompasses several diverse mechanisms by which cells internalize macromolecules and particles into transport vesicles derived from the plasma membrane. The best characterized uptake mechanism is the clathrin-dependent pathway. Nonclathrin mediated mechanisms of endocytosis have also been identified with varying dependency of dynamin, caveolin, and small GTP-binding proteins.[11,12] Both the clathrin-dependent pathway and the clathrin- and dynamin-independent pathways carry their cargo into early endosomes from where it can be further sorted either into the lysosomal pathway, the trans-Golgi network (TGN), or for recycling to the cell surface.

* Corresponding author: Phone: +47 22934293. Fax: +47 22508692. E-mail: Tore-Geir.Iversen@rr-research.no.
† University of Oslo.
‡ Rikshospitalet University Hospital Montebello.
§ University of Copenhagen.

10.1021/nl0803848 CCC: $40.75
Published on Web 06/21/2008

Ricin and Shiga toxins can enter the cells via multiple endocytic pathways some of which are both clathrin- and caveola-independent.[13–15] To study retrograde transport of these toxins, genetically modified toxins containing sulfation and glycosylation sites have been extensively used in biochemical assays exploiting the fact that sulfation is a specific Golgi modification and that glycosylation occurs in the endoplasmic reticulum (ER). Thus, retrograde transport to the Golgi and ER is necessary for the toxins to reach the cytosol where they exert their toxic effect.[13] So far, one has not been able to visualize ricin in the ER. In the present study, the Qdots were coupled to the three different ligands Shiga toxin, ricin, and transferrin to investigate whether their intracellular routing including retrograde transport to the Golgi and the ER were similar to that of the ligands themselves, hence exploring the potential of the Qdots as fluorescent probes. Furthermore, we investigated whether internalization of these Qdot bioconjugates affected intracellular sorting as such.

Preparation of Functional Ligand:Qdot Bioconjugates via the Biotin:Streptavidin Conjugation. The ligand:Qdots were prepared by two approaches: (1) in the tube by mixing biotinylated ligands (transferrin, ShigaB, and ricinB) with streptavidin-coupled Qdots (at molar ratios ligand:QD, 1:1, 5:1, or 10:1), or by (2) generation of the ligand:Qdots at the cell surface of HeLa cells while keeping them at 4 °C (see Supporting Information). Both approaches of preparation resulted in functional Tf:Qdots and ricinB:Qdots that were similarly endocytosed and distributed in the cells irrespective of the ligand:QD ratio. However, ShigaB:Qdot bioconjugates prepared at the cell surface were functional, whereas their preparation in the tube resulted in bioconjugates that were not functional in binding to receptors at the cell surface, probably because of the binding of biotinylated ShigaB to the Qdot in a manner that sterically blocked ShigaB interaction with its receptor. In this study, we have therefore chosen to present the confocal microscopy images of the ligand:Qdots formed at the cell surface.

The hydrodynamic diameter of the streptavidin-coated QD655 (Invitrogen Inc.) was measured by dynamic light scattering (DLS) to be 30 nm, whereas the size of the ricinB:QD655 and the transferrin:QD655 bioconjugates were 26 and 50 nm, respectively (see Supporting Information, Table 1S). Recent studies have shown that spherical gold nanoparticles with a size of approximately 50 nm display a maximum rate of endocytosis[16,17]

Delayed Recycling and Endosomal Accumulation of Transferrin:Qdot Bioconjugates. Internalization of the complex between transferrin (Tf) bound iron and the transferrin receptor (TfR) is the major route of cellular iron uptake. The complexes are constitutively endocytosed by clathrin-dependent/receptor-mediated endocytosis and very efficiently recycled to the plasma membrane (>99%). Tf has also been investigated as a potential ligand for targeted delivery of therapeutic agents that suffer from poor pharmacokinetic properties.[18,19] In this work, we have used confocal fluorescence microscopy to investigate whether endocytosis, intracellular trafficking, and recycling of our Tf:Qdot bioconjugates were similar to that of Tf itself. HeLa cells were chosen as target cells since they are known to have a high number of TfR. Figure 1A shows that the Tf:Qdot bioconjugates were internalized efficiently within 15 min with kinetics similar to transferrin (panel a,b). Furthermore, endocytosis experiments using the HeLa K44A cells, with a tetracycline-induced expression of a dominant-negative dynamin mutant, revealed that the Tf:Qdots were internalized by dynamin-dependent endocytosis, similar to Tf (Figure 1A, panel c,d). Upon expression of mutant dynamin (−tetracycline for 48 h), the Tf:Qdots still remained at the cell surface after allowing their endocytosis for 30 min (panel d). To further prove that functional Tf:Qdots were formed and specifically targeted for internalization through the Tf−TfR interaction, two control experiments were performed: First, the cells were incubated with unconjugated Qdots. In the second experiment, the cells were saturated with free Tf for 30 min to block the available TfRs on the cell surface, followed by endocytosis of Tf:Qdots formed in the tube. In both cases, cells displayed minimal fluorescence from the Qdots in the confocal microscope (data not shown).

After 15−30 min of endocytosis, the Tf:Qdot bioconjugates displayed good overlap with early endosomal markers such as early endosomal antigen 1 (EEA1) and TfR (Figure 1A, panel a,b). After chasing of their endocytosis for 3−4 h, they accumulated in more perinuclear endosomes, displaying less colocalization with TfR and only little colocalization with lysosomal markers such as Lamp-1 and CD63 (Figure 1B, panel a,b). Thus, most of the Tf:Qdots did not accumulate in lysosomes. Moreover, even after chasing the Tf:Qdots for more than 4 h, their fluorescence intensity still remained at the same level indicating no significant recycling. In a recent paper, Tf-receptor-mediated uptake of quantum rod (QR)-Tf conjugates has also been reported,[9] but because the uptake was studied with QR-Tf continuously present in the medium and not by performing a "pulse-chase" type of uptake, nothing could be concluded about their kinetics of recycling/exocytosis. It has been shown that Tf conjugated to polymeric nanoparticles recycled at a much slower rate than Tf itself and resulted in greater intracellular retention of Tf-conjugated NPs as compared with the unconjugated NPs.[20] In a recent study, using transferrin-coated gold nanoparticles (NPs), it was found that NPs were exocytosed in a linear relationship to size, and it was further suggested that most of the Tf−gold NPs ended up in late endosomes/lysosomes from where they recycled/exocytosed.[21] Thus, these Tf−nanoparticle bioconjugates seem to follow a different recycling route than the normal transferrin.

After endocytosis of Tf:Qdots for 2 h, we allowed fluorescently alexa488-labeled transferrin to be endocytosed for 20 min in HeLa K44A cells (Figure 1B, panel c,d). In the control cells not induced to express mutant dynamin (+tetracycline), only partial overlap was observed between the accumulated Tf:Qdots and the alexa488-Tf, indicating that tranferrin was not transported into or trapped in these endosomes (Figure 1B, panel c). In these cells, further chasing of alexa488-Tf for 30 and 60 min showed recycling out of the cells at a rate comparable to cells without Tf:

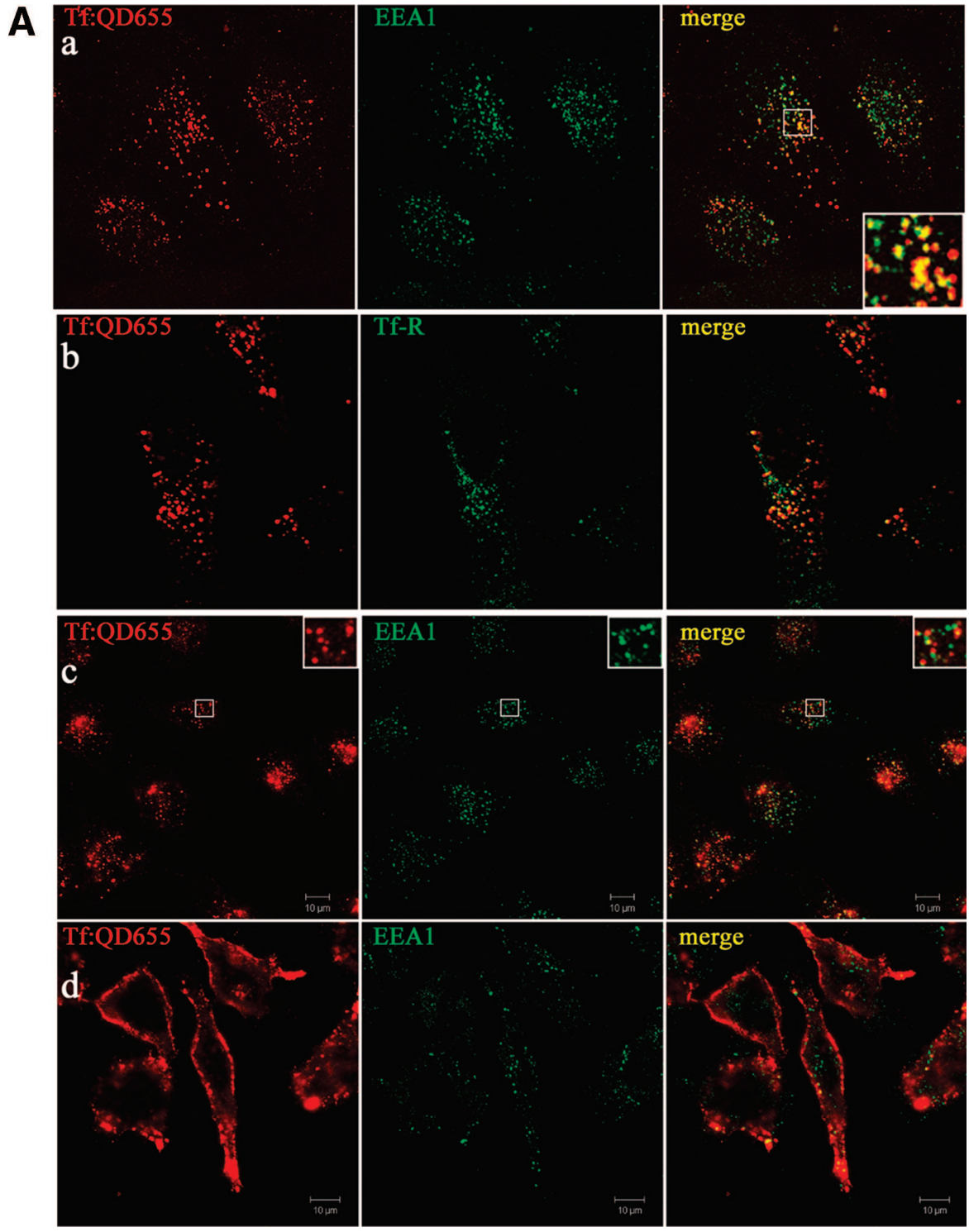

Figure 1. (A) Intracellular location of transferrin (Tf):quantum dot (QD655) bioconjugates in live HeLa cells. The Tf:QD655 bioconjugates were constituted and bound to the cell surface at 4 °C, and then allowed to be internalized into the cells for various times at 37 °C. The cells were then fixed and prepared for immunofluorescence microscopy labelling them with antibodies against EEA1 and Tf-R and with the appropriate secondary ab-Cy2 conjugates. Tf:QDs internalized for 15 min colocalized partly with EEA1 and the TfR (a,b). Endocytosis of the Tf:QD655s for 30 min in the HeLa dynK44A cell line (c,d): Images show the dynamin-dependent uptake of surface-bound Tf:QD655 with normal uptake in control cells (c) and no uptake in the mutant dynamin expressing cells (d, induced for 48 h, −tetracycline). Yellow in the merged images indicates colocalization. Bars, 10 μm. (B) Intracellular accumulation of Tf:QD655 bioconjugates after endocytosis for 3 h in HeLa cells. Tf:QD655s are retained in endosomes that partly colocalize with TfR and CD63 (a,b). Dynamin-dependent endocytosis and accumulation of Tf:QD655 into perinuclear clusters of endosomes in HeLa K44A cells (c,d): Tf:QD655 bound at the cell surface at 4 °C were endocytosed at 37 °C for 2 h, with addition of alexa488-transferrin for the last 20 min. Images shows the *z*,*x* section (upper panel) and the *z*,*y*section (right panel) cutting orthogonally through the cell obtained from *z*-stack image series of the cells. In the uninduced control cells (+tet), the Tf:Qdots were observed in perinuclear endosomal clusters inside the cell. In the cells with induced mutant dynamin (−tet), the Tf:Qdots localized along the periphery of the cell. Bars, 10 μm.

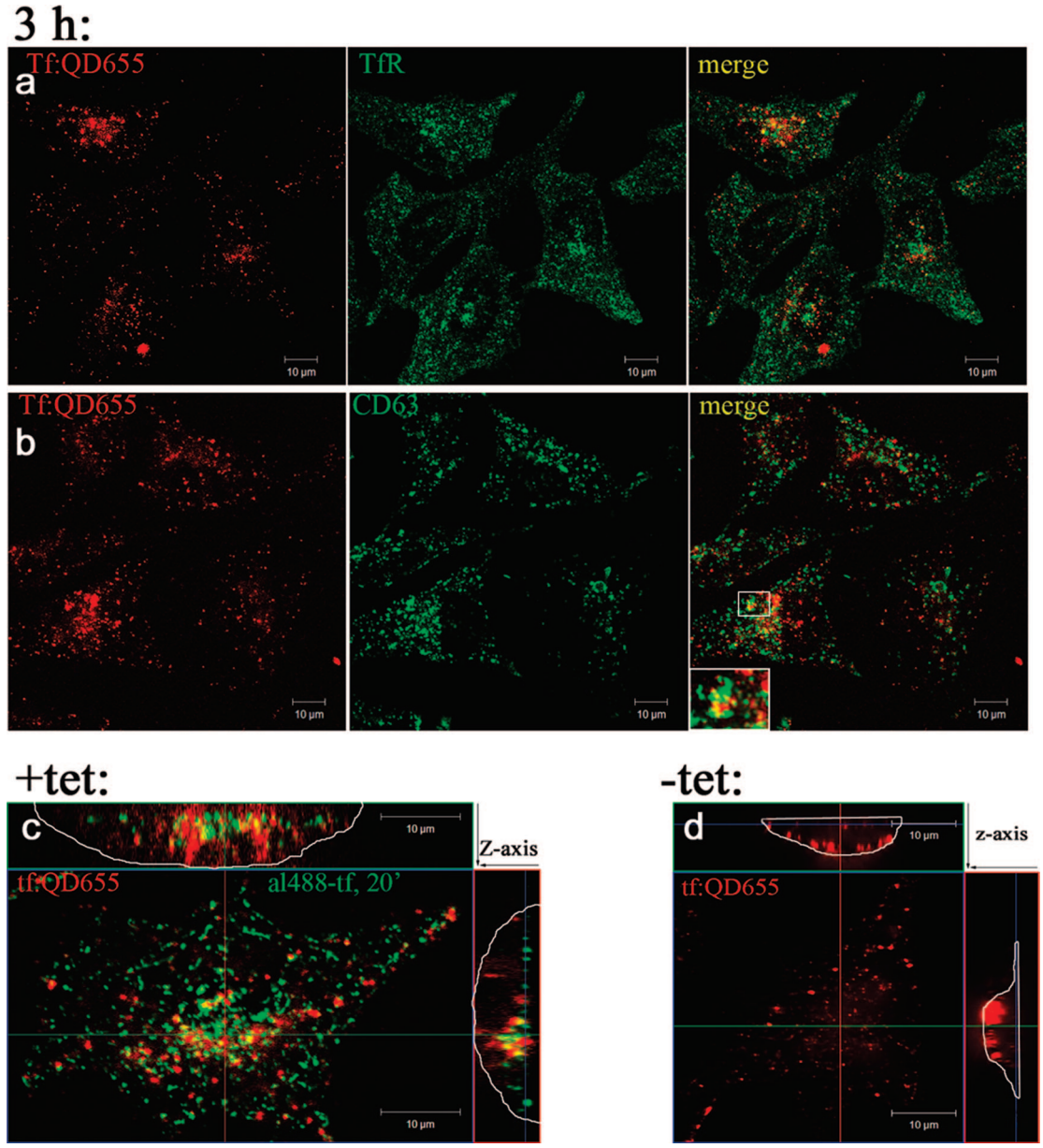

Figure 1. Continued.

Qdots and with no detectable alexa488-Tf trapped in the Tf:Qdot positive endosomal compartments (data not shown). Thus, recycling of transferrin was not significantly delayed by the accumulation of Tf:Qdot bioconjugates. Moreover, when the cells were induced (−tetracycline) to express mutant dynamin, the Tf:Qdots remained at the cell surface occupying the Tf receptors and also causing a strongly reduced binding of alexa488-Tf to the cells (Figure 1B, panel d).

No Transport of the ShigaB:Qdots and RicinB:Qdots to the Golgi Apparatus. After being endocytosed, a fraction of Shiga toxin and ricin is routed from endosomes and into the Golgi apparatus and further retrogradely transported to the endoplasmatic reticulum from where they are translocated into the cytosol exerting their toxic effect.[22,23] By fluorescence microscopy, a fraction of Shiga toxin and ricin has been visualized overlapping with Golgi markers such as TGN46 and giantin.[24,25]

ShigaB:Qdots were prepared at the plasma membrane of HeLa cells incubated at 4 °C, by the binding of biotinylated ShigaB followed by washings and binding of streptavidin-coupled Qdots. Figure 2 shows endocytosis of the ShigaB:Qdots at 37 °C for 30 and 90 min, respectively. Early in the endocytic/intracellullar process (until 30 min), we observed that ShigaB:Qdot bioconjugates displayed overlap with EEA1-positive endosomes (panel c). After 90 min of endocytosis, less overlap with EEA1-positive structures was observed (panel d) indicating their further transport and accumulation into other endosomes dispersed throughout the cytoplasm. Furthermore, whereas a fraction of the ShigaB subunit clearly displayed overlap with TGN46 already after 30 min of endocytosis (panel a), no such colocalization of the ShigaB:Qdots with TGN46 in perinuclear structures was observed even after 90 min of endocytosis (panel e).

We also studied the internalization and intracellular trafficking of ricinB:Qdots constituted at the cell surface of

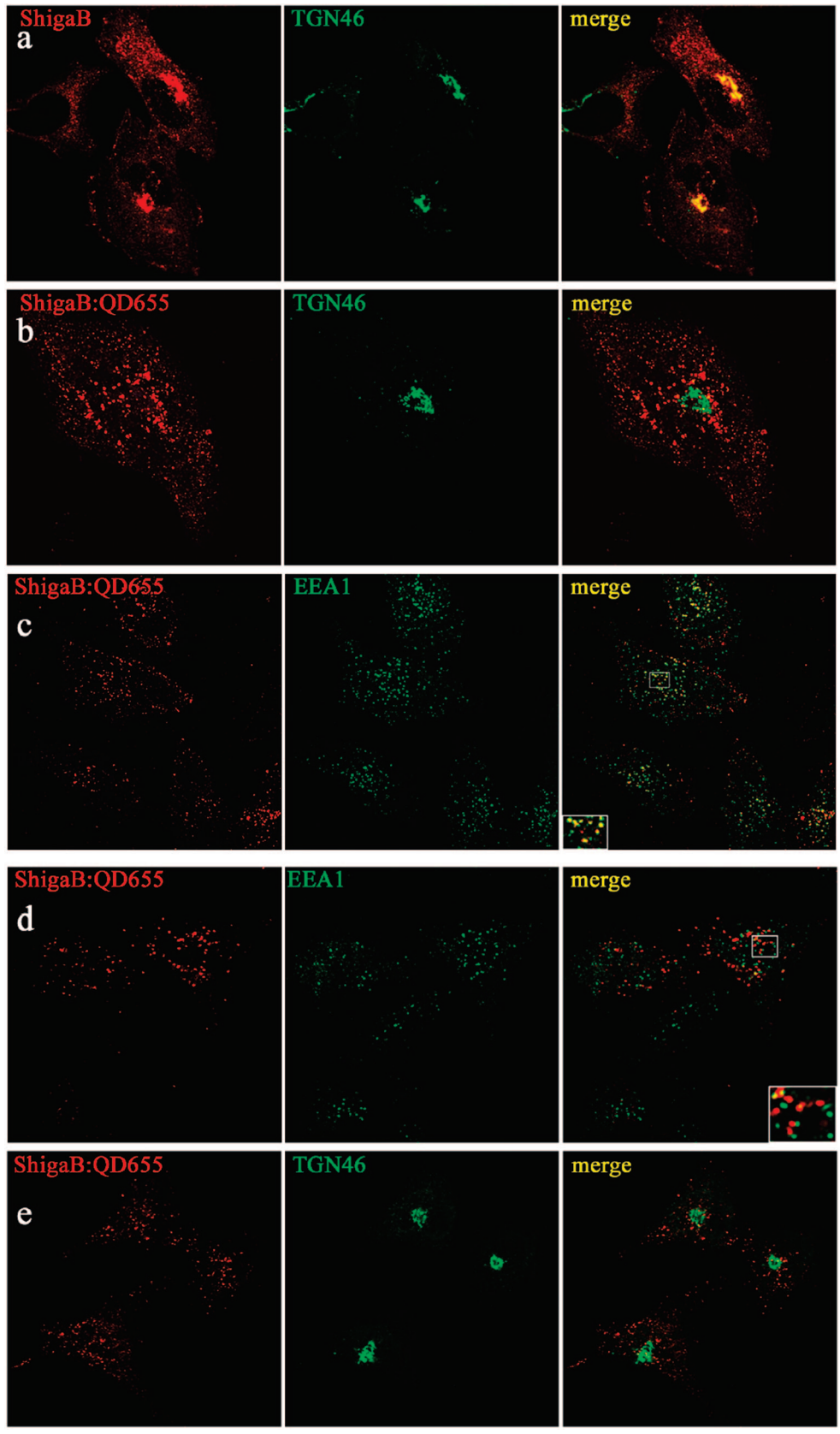

Figure 2. Blocked transport of the ShigaB:Qdot bioconjugate into the trans-Golgi network. The ShigaB:Qdot bioconjugates were constituted on the cell surface at 4 °C prior to endocytosis (37 °C). After endocytosis for 30 min, the ShigaB-subunit was observed colocalizing with the TGN-marker TGN46 (a), but no colocalization of ShigaB:QD655 with TGN46 was observed (b). ShigaB:QD655 colocalizes with EEA1 in peripheral endosomes (panel c; yellow in inset). After uptake for 90 min, less colocalization between ShigaB:QD655 and EEA1 was observed (d), and colocalization of ShigaB:QD655 with TGN46 was still not observed (e). Bars, 10 μm.

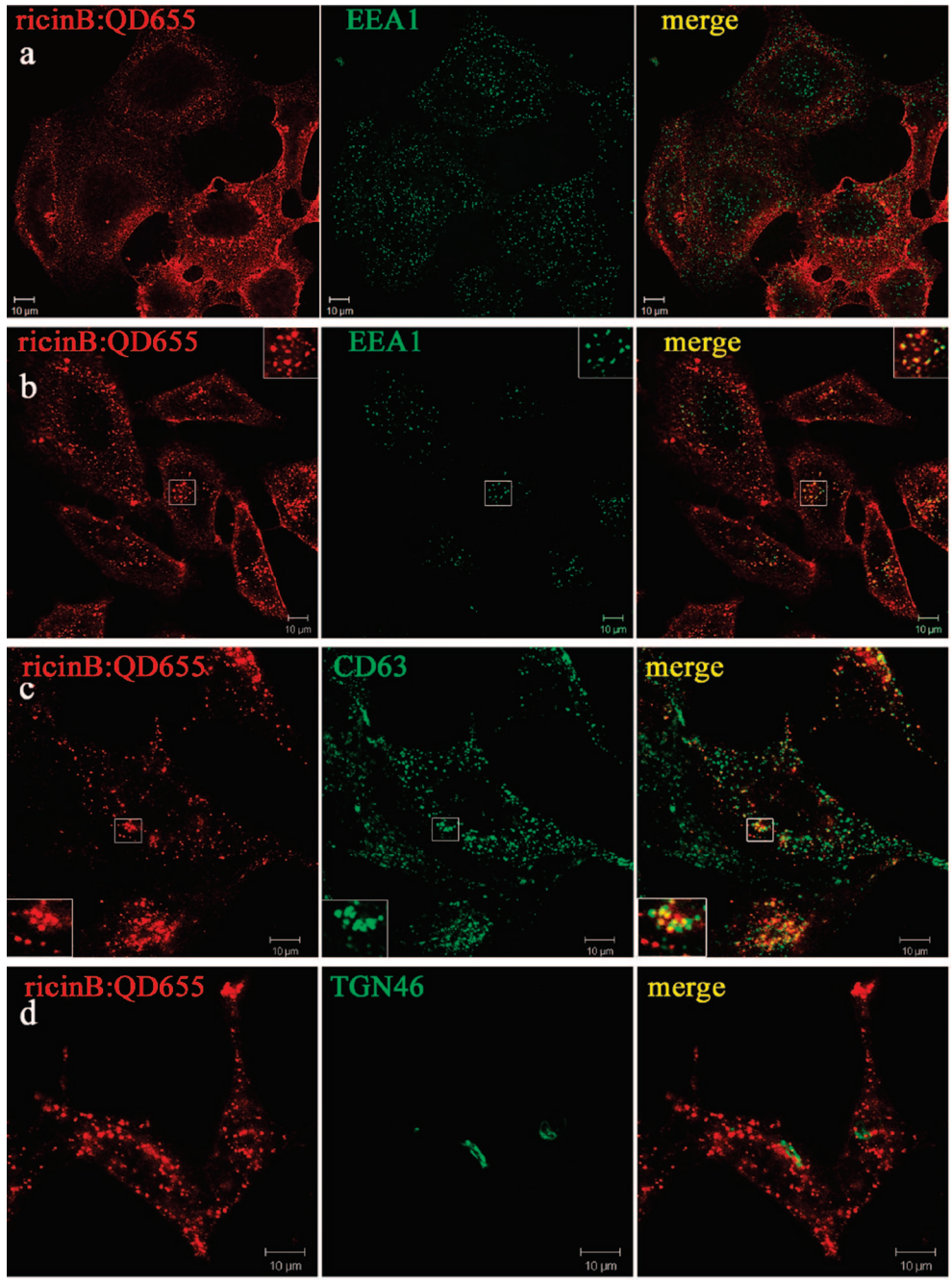

Figure 3. Intracellular accumulation of ricinB:QD655 bioconjugates after endocytosis in HeLa cells. Upper panel (a) shows binding of ricinB:QD655 to the cell surface on ice. Endocytosis of ricinB:QD655 for 30 min, and overlapping staining with EEA1 (b). Endocytosis for 180 min, with the ricinB:QD655 bioconjugates displaying partial colocalization with lysosomal marker CD63 (c), but not with TGN46 (d). Bars, 10 μm.

HeLa cells. Figure 3 shows that the ricinB:Qdot bioconjugates displayed overlap with EEA1-positive endosomes after 30 min of endocytosis (panel b), while upon longer times of endocytosis (180 min) they were routed further into more perinuclear vesicles displaying partial overlap with CD63 (panel c). However, most of these ricinB:Qdot-positive vesicular structures did not stain positive for lysosomal markers. The ricinB:Qdots remained accumulated in these endosomes for >24 h (data not shown). Recently, cholera toxin subunit B (CTB)-quantum dot conjugates have been found to be internalized into small dispersed vesicles of the cells where they retained for several days.[26] Furthermore, whereas a fraction of ricin has been visualized in the Golgi apparatus within 3 h of endocytosis,[27] no significant colocalization of ricin:Qdots with the trans-Golgi marker TGN46 was observed (panel d). The finding that ligands bound to Qdots are not transported to the Golgi apparatus is reminiscent of results showing that ricin coupled to gold particles and in polyvalent ricin conjugates with HRP ended up in locations other than the Golgi.[28] In future studies, it would be interesting to further characterize the nature of the vesicles where Qdots are accumulating and to study whether this endosomal accumulation could be changed by manipulating the number of ligands per particle (valency) or the conditions

in the cell. It should be mentioned that endocytosis for 4 h of ricinB:Qdots prepared with either a 1:1 or 5:1 molar ratio of ricinB:Qdot displayed a similar endosomal distribution in the cells (data not shown).

For all three ligand:QD bioconjugates, we tested if the uptake was specific (through respective receptors) or if macropinocytosis was involved. We exposed the cells to 100 μM 5-(*N*-ethyl-*N*-isopropyl) amiloride (EIPA; inhibitor of macropinocytosis) prior to addition of the bioconjugates, but no changes in endocytosis were seen with respect to the control indicating other types of endocytosis (results not shown). Furthermore, the cellular uptake of the three ligand:Qdot bioconjugates were greatly enhanced compared with uptake of the unconjugated Qdots, as estimated by measuring and comparing fluorescence intensities in the confocal microscope. In our endocytosis experiments, the concentration of the ligand:Qdots added to the cells varied from 5 to 20 nM. No fluorescence from the Qdots were observed in control experiments when allowing endocytosis of unconjugated Qdots (5−20 nM) for the same time periods as the ligand:Qdot bioconjugates.

Ricin:QD Bioconjugates Affect the Intracellular Trafficking of Unconjugated Ricin and Shiga Toxin. To investigate whether transport of ricin and Shiga toxin from endosomes to the TGN was affected by the endosomal accumulation of ricinB:QDs, we measured sulfation of the modified ricin sulf-1 and ShigaB sulf-2, respectively. Figure 4A shows that the sulfation of ricin sulf-1 was inhibited in cells where ricinB:Qdots had accumulated intracellularly for 24 h, displaying a >70% reducion as compared with control cells. Control experiments using ^{125}I-ricin to quantify endocytic uptake revealed that this result was not due to a reduced uptake of ricin sulf-1 (data not shown). Preincubation with ricin:QDs for 3 h also gave a reduction in the sulfation of ricin sulf-1, but this result could be attributed to the concomitant reduction in endocytosis of ^{125}I-ricin also observed. Furthermore, exposure of the cells with ricinB:QD bioconjugates for 24 h revealed no significant changes in protein synthesis or cytotoxicity effects in a MTT assay performed (data not shown). Together, this result indicated that the ricinB:Qdot bioconjugates caused obstruction in an endosome-to-Golgi transport pathway, and hence the natural transport of ricin was affected. For Shiga sulf-2, the effect was opposite, as a two- to threefold stimulation in the transport was detected after 3 h preincubation with ricin:Qdots; see Figure 4B. An explanation could be that blockage of one pathway to the Golgi apparatus caused by the accumulation of ricinB:Qdots will induce a compensatory increase of other pathways, into which the transport of Shiga is directed.

In this work, we have investigated whether Qdots coupled to Shiga toxin, ricin, and transferrin serve as relevant intracellular ligand probes. All three ligand:Qdot bioconjugates were endocytosed specifically via binding to their receptors. It appears that the Qdot bioconjugates are retained in endocytic structures and not efficiently exocytosed or routed further to the Golgi apparatus. We speculate that the size of the ligand:Qdots (30−50 nm)

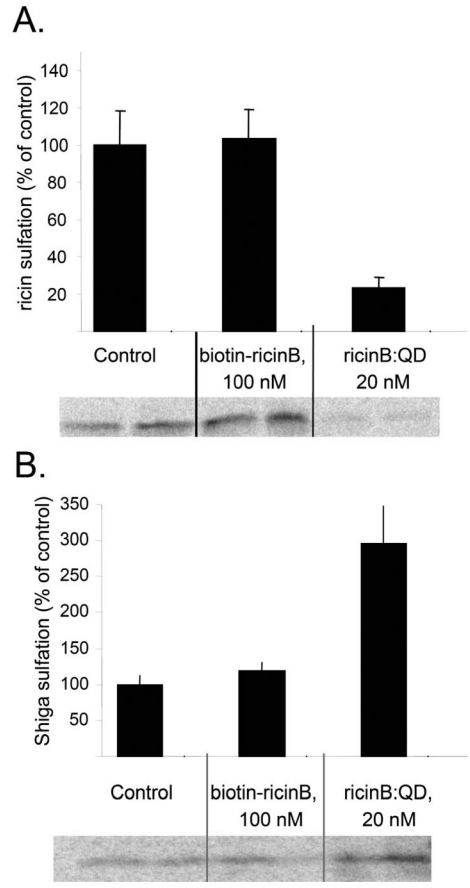

Figure 4. Ricin sulf-1 (A) and Shiga sulf-2 (B) sulfation following accumulation of ricinB:QD655. HeLa cells were allowed to endocytose ricinB:QD655 for 24 h prior to the ricin sulfation and for 3 h prior to the ShigaB sulfation experiment. The cells were then incubated for 3 h at 37 °C in DMEM containing $Na^{35}SO_4$ (200 μCi/ml) followed by the addition and further incubation at 37 °C of either ricin sulf-1 for 2 h, or ShigaB sulf2 for 1 h. The cells were washed (with 0.1 M lactose in ricin sulfation), lysed, and proteins were immunoprecipitated with a rabbit antiricin ab. or a mouse-anti-Shiga ab. Following SDS−PAGE, gels were dried, and signals were detected using a PhosphoImager screen. Band intensities were quantified using the ImageQuant 5.0 software.

used in this study prevents them from following the same endocytic pathways as their respective ligands. Importantly, accumulation of the ricinB:Qdots perturbed the intracellular routing of unconjugated ricin and Shiga toxin to the Golgi apparatus, whereas the endocytosis and recycling of transferrin seemed unaffected by endosomal accumulation of Tf:Qdots. Thus, for the first time, we have demonstrated that endosomal accumulation of a ligand:nanoparticle bioconjugate can induce changes in the normal intracellular transport of unconjugated ligands. In our further studies, we plan to investigate whether the intracellular transport of smaller ligand:Qdot bioconjugates will be more in accordance with that of the ligand. We intend to extend our studies of the dynamics of intracellular trafficking of Qdots and other nanoparticle bioconjugates, particularly to determine the influence of different sizes and surface properties of NPs on their endocytic uptake and sorting into different intracellular compartments. The use of Qdots may have severe consequences

on cell physiology, and thus more knowledge about the endocytic pathways and their influence on intracellular distribution of NPs will be important for developing nanoparticles into efficient intracellular probes and delivery vehicles.

Acknowledgment. We thank Andrew Jones at Malvern Instruments Inc. for expert technical assistance. C.T. and T.-G.I. are the recipients of predoctoral and career fellowships, respectively, from the FUGE and NANOMAT programmes. This work was supported by the Research Council of Norway.

Supporting Information Available: Materials and methods section with description of cell culture, preparation of functional Qdot-streptavidin:biotinylated-ligand bioconjugates, hydrodynamic diameter measurements by dynamic light scattering, laser scanning fluorescence microscopy, and ricin and Shiga sulfation assay for assessing intracellular transport into the Golgi apparatus. This material is available free of charge via the Internet at http://pubs.acs.org.

References

(1) Alivisatos, A. P.; Gu, W.; Larabell, C. *Annu. Rev. Biomed. Eng.* **2004**, n/a.
(2) Michalet, X.; Pinaud, F. F.; Bentolila, L. A.; Tsay, J. M.; Doose, S.; Li, J. J.; Sundaresan, G.; Wu, A. M.; Gambhir, S. S.; Weiss, S. *Science* **2005**, *307*, 538–544.
(3) Gao, X.; Cui, Y.; Levenson, R. M.; Chung, L. W.; Nie, S. *Nat. Biotechnol.* **2004**, *22*, 969–976.
(4) Lewinski, N.; Colvin, V.; Drezek, R. *Small* **2008**, *4*, 26–49.
(5) Maysinger, D.; Lovric, J.; Eisenberg, A.; Savic, R. *European Journal of Pharmaceutics and Biopharmaceutics* **2007**, *65*, 270–281.
(6) Dahan, M.; Levi, S.; Luccardini, C.; Rostaing, P.; Riveau, B.; Triller, A. *Science* **2003**, *302*, 442–445.
(7) Lidke, D. S.; Nagy, P.; Heintzmann, R.; rndt-Jovin, D. J.; Post, J. N.; Grecco, H. E.; Jares-Erijman, E. A.; Jovin, T. M. *Nat. Biotechnol.* **2004**, *22*, 198–203.
(8) Lidke, D. S.; Lidke, K. A.; Rieger, B.; Jovin, T. M.; rndt-Jovin, D. J. *J. Cell Biol.* **2005**, *170*, 619–626.
(9) Yong, K. T.; Qian, J.; Roy, I.; Lee, H. H.; Bergey, E. J.; Tramposch, K. M.; He, S.; Swihart, M. T.; Maitra, A.; Prasad, P. N. *Nano Lett.* **2007**, *7*, 761–765.
(10) Bharali, D. J.; Lucey, D. W.; Jayakumar, H.; Pudavar, H. E.; Prasad, P. N. *J. Am. Chem. Soc.* **2005**, *127*, 11364–11371.
(11) Mayor, S.; Pagano, R. E. *Nat. Rev. Mol. Cell Biol.* **2007**, *8*, 603–612.
(12) Sandvig, K.; Torgersen, M. L.; Raa, H. A.; van Deurs, B. *Histochem. Cell Biol.* **2008**, *129*, 267–276.
(13) Sandvig, K.; van Deurs, B. *Gene Ther.* **2005**, *12*, 865–872.
(14) Johannes, L.; Decaudin, D. *Gene Ther.* **2005**, *12*, 1360–1368.
(15) Sandvig, K.; Grimmer, S.; Lauvrak, U.; Torgersen, L.; Skretting, G.; van Deurs, B.; Iversen, T.-G. *Histochem. Cell Biol.* **2002**, *117*, 131–141.
(16) Gao, H.; Shi, W.; Freund, L. B. *Proc. Natl. Acad. Sci U.S.A.* **2005**, *102*, 9469–9474.
(17) Chithrani, B. D.; Ghazani, A. A.; Chan, W. C. W. *Nano Lett.* **2006**, *6*, 662–668.
(18) Yang, P. H.; Sun, X.; Chiu, J. F.; Sun, H.; He, Q. Y. *Bioconjug. Chem.* **2005**, *16*, 494–496.
(19) Qian, Z. M.; Li, H.; Sun, H.; Ho, K. *Pharmacol. Rev.* **2002**, *54*, 561–587.
(20) Sahoo, S. K.; Labhasetwar, V. *Mol. Pharm.* **2005**, *2*, 373–383.
(21) Chithrani, B. D.; Chan, W. C. *Nano Lett.* **2007**, *7*, 1542–1550.
(22) Sandvig, K.; Garred, O.; Prydz, K.; Kozlov, J. V.; Hansen, S. H.; van Deurs, B. *Nature* **1992**, *358*, 510–512.
(23) Rapak, A.; Falnes, P. O.; Olsnes, S. *Proc. Natl. Acad. Sci. U.S.A.* **1997**, *94*, 3783–3788.
(24) Utskarpen, A.; Slagsvold, H. H.; Iversen, T. G.; Walchli, S.; Sandvig, K. *Traffic* **2006**, *7*, 663–672.
(25) Torgersen, M. L.; Walchli, S.; Grimmer, S.; Skanland, S. S.; Sandvig, K. *J. Biol. Chem.* **2007**, *282*, 16317–16328.
(26) Chakraborty, S. K.; Fitzpatrick, J. A. J.; Phillippi, J. A.; Andreko, S.; Waggoner, A. S.; Bruchez, M. P.; Ballou, B. *Nano Lett.* **2007**, *7*, 2618–2626.
(27) Lauvrak, S. U.; Llorente, A.; Iversen, T. G.; Sandvig, K. *J. Cell Sci.* **2002**, *115*, 3449–3456.
(28) van Deurs, B.; Tonnessen, T. I.; Petersen, O. W.; Sandvig, K.; Olsnes, S. *J. Cell Biol.* **1986**, *102*, 37–47.

NL0803848